Geometrical dependence of the electrical properties of H+ 3

Joseph D. Augspurger and Clifford E. Dykstra

Citation: The Journal of Chemical Physics **88**, 3817 (1988); doi: 10.1063/1.453882
View online: http://dx.doi.org/10.1063/1.453882
View Table of Contents: http://scitation.aip.org/content/aip/journal/jcp/88/6?ver=pdfcov
Published by the AIP Publishing

Geometrical dependence of the electrical properties of H_3^+

Joseph D. Augspurger and Clifford E. Dykstra
Department of Chemistry, University of Illinois, Urbana, Illinois 61801

(Received 30 October 1987; accepted 2 December 1987)

Ab initio calculations using large basis sets with self-consistent field and fully correlated wave functions have been carried out to examine the geometry dependence of multipole moments, polarizabilities, and hyperpolarizabilities of H_3^+. These surfaces of properties were continued to the H^+–H_2 dissociation limit in order to demonstrate the change in the properties of H_2 upon protonation. There is generally a decrease in the polarizability upon protonation, though at long range the proton's interaction with H_2 produces a general increase. The implications of this on vibrational state properties are considered.

INTRODUCTION

The past ten years have seen steady progress in the detailed theoretical and spectroscopic understanding of H_3^+, a prototypical cationic species. The vibrational states and transition frequencies have been the focus of interest, and to this end there have been several potential energy surfaces developed, including those by Carney and Porter,[1] Dykstra and Swope,[2] Burton *et al.*,[3] and Meyer *et al.*[4] In 1980 Oka[5] reported the first experimental rovibrational transitions, definitely identifying the fundamental asymmetric stretch to be 2521.6 cm^{-1} and reporting several other transitions, though without definite assignments initially. That spurred many attempts to treat the complete vibrational problem of H_3^+, including the studies by Burton *et al.*,[3] Meyer *et al.*,[4] Carney *et al.*,[1,6–8] Martire and Burton,[9] Tennyson and Sutcliffe,[10] and Hamilton.[11] There has been extremely good success in the calculation of the fundamental vibrations of H_3^+ and its isotopomers. Carney *et al.*,[8] using a fit of the Dykstra–Swope surface,[2] found agreement with experimental values[5,12] to about 1 cm^{-1}. Meyer *et al.*[4] reported a standard deviation of less than a wave number between measured and computed values. Further discussion of the progress on the vibrational spectrum of H_3^+ is given in the reports by Carney *et al.*[8] and Meyer *et al.*[4]

The purpose of this report is to examine in detail the electrical properties of H_3^+. H_3^+ is the simplest species from which to understand how protonation affects subtle properties of the electronic wave function such as polarizabilities. Knowledge of the electrical properties of H_3^+ makes it possible to examine the purely electrical part of its interaction with neutral molecules and to isolate the role of that interaction in the energetics of clustering around a cationic species. The specific information that is sought for this purpose is the dependence of the electrical properties on the geometrical parameters of H_3^+. To do this accurately, attention must be given to the effect of correlation on the permanent moments and polarizabilities, and to basis set quality. The first work of this sort was the *ab initio* investigation of the dipole and second moment surfaces by Carney and Porter.[13]

Comparison of H_3^+ property surfaces with H_2 properties at equilibrium is useful in seeing how a cation's properties differ from those of a similar neutral. The benchmark treatment of H_2 done by Kolos, Wolniewicz, and Roothaan in the 1960's has provided an essentially exact potential energy curve,[14] vibrational state energies,[15] quadrupole moments,[16] and dipole polarizabilities.[17] There have been many reports since, including in some cases the vibrational contribution to the polarizabilities.[18–25] At an internuclear distance of 1.4 a.u., Kolos and Wolniewicz calculated parallel and perpendicular dipole polarizabilities of 6.380 49 and 4.577 69 a.u. Dykstra,[26] using derivative Hartree–Fock theory,[27] has calculated all dipole and quadrupole properties through the hyperpolarizabilities. Bishop and Lam[20] have calculated the static and vibrational contributions of the electrical properties through the octupoles up to the second hyperpolarizabilities. A complete set of moments, polarizabilities, and hyperpolarizabilities through fourth rank Cartesian tensors has been reported for equilibrium H_2 by Maroulis and Bishop.[28]

THEORETICAL APPROACH

The primary basis set consisted of 60 Gaussian basis functions, with 20 centered at each nucleus. The contraction coefficients and the exponents of this basis set are given in Table I. The core *s* functions were taken from Huzinaga,[29] and the *p* and *d* functions are very similar to those used by Dykstra and Swope.[2] Basis set limitations are discussed in the Appendix. Moments, polarizabilities, and hyperpolarizabilities were calculated analytically for H_3^+ at the SCF level with the derivative Hartree–Fock approach (DHF).[27]

TABLE I. Basis set.

Function types	Exponents	Contraction coefficients
s	148.273 2	0.000 97
	22.174 27	0.007 53
	4.970 178	0.039 39
	1.370 178	1.0
	0.436 661	1.0
	0.155 858	1.0
	0.060 738	1.0
p	1.6	1.0
	0.5	1.0
	0.15	1.0
d	1.33	1.0

 0021-9606/88/063817-09$02.10

DHF is an open-ended, uniform method for calculating properties corresponding to derivatives of the energy. Here it is applied to obtain the electrical properties which are derivatives with respect to electric field and field gradient components. To include correlation effects, finite field calculations were performed with full configuration interaction (CI). This was done using the method of self-consistent electron pairs (SCEP)[30] in the same manner as in the H_3^+ potential surface calculation by Dykstra and Swope,[2] where the reference configuration was constructed from a Brueckner orbital. This special treatment is strictly equivalent to full CI for the two electron system.

In the finite field calculations, the effect of a field or field gradient was included by computing the appropriate one electron multipole-moment component operator, multiplying it by the desired field or field gradient strength, and adding it to the kinetic energy/nuclear attraction one-electron operator matrix before calculating SCF and SCEP wave functions and energies. The correlated moments and polarizabilities were calculated by fitting these SCEP energies to a polynomial of powers of the field or field gradient by a linear least squares procedure. To assure numerical significance, the polynomials were at least two orders greater than that required to obtain the property desired. This procedure was checked by fitting the corresponding SCF energies to the same order polynomials and comparing those property values against the analytical DHF values. The error due to fitting and numerical limitations of the finite field treatment should not exceed 0.01% for the permanent moments and dipole polarizabilities and 1% for the quadrupole polarizabilities and for the hyperpolarizabilities on the basis of these comparisons. Typical field and field gradient strengths were 0.01 a.u.

The conventions used for the electrical properties are the following.[31] All are in a.u. and all are derivatives of the energy with respect to field and field gradient components. The conversion from a.u. to SI units is $4.486\,584\times10^{-40}$ C m^2 per a.u. for a quadrupole or second moment, and $1.648\,778\times10^{-41}$ C^2 m^2 J^{-1} per a.u. for a dipole polarizability. All properties are in Cartesian form, or traced form, not spherical or traceless. Relationships between the Cartesian forms and the traceless forms have been presented by Applequist,[32] and expressions relevant to this study are given in Table II. Moments are designated as M, and for example $M_{xy} = 1/2\Sigma q_i x_i y_i$. Polarizabilities are designated as P with subscripts corresponding to appropriate moment elements. Properties designated other than with M or P have been converted so that other often-used conventions apply.

TABLE II. Relations of electrical properties from Cartesian form to traceless form.[a]

μ_α	$= M_\alpha$
$\Theta_{\alpha\beta}$	$= 3M_{\alpha\beta} - \delta_{\alpha\beta}M_{\nu\nu}$
$\alpha_{\alpha\beta}$	$= -P_{\alpha,\beta}$
$A_{\alpha\beta\gamma}$	$= -(3P_{\alpha,\beta\gamma} - \delta_{\beta\gamma}P_{\alpha,\nu\nu})$
$C_{\alpha\beta\gamma\delta}$	$= -(3P_{\alpha\beta,\gamma\delta} - \delta_{\alpha\beta}P_{\nu\nu,\gamma\delta} - \delta_{\gamma\delta}P_{\alpha\beta,\nu\nu} + \frac{1}{3}\delta_{\alpha\beta}\delta_{\gamma\delta}P_{\nu\nu,\mu\mu})$
$\beta_{\alpha\beta\gamma}$	$= P_{\alpha,\beta,\gamma}$
$\gamma_{\alpha\beta\gamma\delta}$	$= -P_{\alpha,\beta,\gamma,\delta}$

[a]These formulas use repeated index summation convention, e.g., $C_{xx,xx} = -\frac{1}{3}[4P_{xx,xx} - P_{yy,yy} - P_{zz,zz} - 4(+P_{xx,zz}) + 2P_{yy,zz}]$.

The equilibrium geometry of H_3^+ is an equilateral triangle with a H–H bond distance of 1.6504 a.u.[2] In the coordinate system used here, the origin coincides with the center of mass, and one proton lies on the positive x axis. The z axis is perpendicular to the molecular plane. S' is the distance from the origin to any of the protons, and is equal to the bond distance divided by the square root of three. S'_{eq} is 0.952 858 88 a.u. All electrical properties are calculated with respect to the coordinate origin. A specific geometrical point on the surface is given by values of three coordinates, S, R, and θ, in the same manner as used by Dykstra and Swope.[2] S, which refers to the symmetric stretching coordinate, is defined as

$$S = S' - S'_{eq}.$$

The two asymmetric stretching coordinates, A_1 and A_2, may be converted to polar form, R and θ, according to the following relations:

$$R^2 = A_1^2 + A_2^2, \quad \tan 3\theta = A_1/A_2.$$

The S, A_1, and A_2 unit displacement vectors are shown in Fig. 1. $\theta = 0°$ corresponds to pure A_1 motion, $\theta = 30°$ to pure A_2 motion, $\theta = 60°$ to pure $-A_1$, and $\theta = 90°$ to pure $-A_2$. This coordinate system has a period of $\theta = 120°$, but since A_2 is equivalent to $-A_2$, $\theta = 0°$ to 60° contains all unique configurations.

Treating the symmetric stretch as separable from the asymmetric stretch facilitated an examination of the vibrational influence on the electrical properties. A method that has been recently developed by Dykstra and Malik, derivative Numerov Cooley (DNC),[33] was used to calculate the electrical properties of several low lying symmetric-stretch vibrational states of H_3^+. DNC solves the difference equations that correspond to the derivative vibrational Schrödinger equation. This can be done to any order of differentiation with any set of parameters, such as field and field gradient strength. The results are analytical values of properties, such as dipole polarizability tensor components, for individual electronic–vibrational states. Effects of rotational motion were not considered. Electronic state values for the properties at specific geometries are those obtained from the *ab initio* SCF or SCEP calculations. The symmetric stretch potential was generated from fitting SCEP energies at eight geometries to a sixth order polynomial in S'. For the six geometries given in Table III, the electronic state properties through the second hyperpolarizabilities were fitted to quadratic polynomials, and these polynomials were used in the

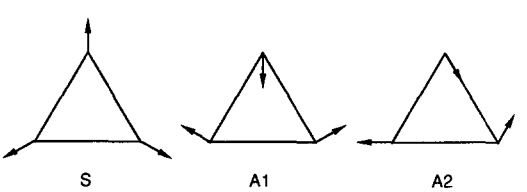

FIG. 1. Displacement vectors from equilibrium configuration.

TABLE III. Symmetric stretch properties (in a.u.) of H_3^+.

S' (a.u.)	0.75	0.88	S'_{eq}	1.02	1.15	1.30
M_{xx}	−0.5763	−0.6931	−0.7636	−0.8318	−0.9731	−1.1517
M_{zz}	−0.4517	−0.5157	−0.5517	−0.5850	−0.6491	−0.7221
$P_{x,x}$	−2.1801	−3.0296	−3.5978	−4.1854	−5.5123	−7.3851
$P_{z,z}$	−1.5277	−1.9710	−2.2454	−2.5143	−3.0753	−3.7809
$P_{x,xx}$	−0.0708	−0.1401	−0.1978	−0.2663	−0.4524	−0.7836
$P_{xx,xx}$	−0.6156	−0.9474	−1.1875	−1.4494	−2.0863	−3.0795
$P_{xx,yy}$	−0.0679	−0.0754	−0.0743	−0.0680	−0.0362	0.0479
$P_{xx,zz}$	−0.1112	−0.1588	−0.1911	−0.2249	−0.3028	−0.4159
$P_{xy,xy}$	−0.2739	−0.4360	−0.5566	−0.6907	−1.0250	−1.5637
$P_{xz,xz}$	−0.2198	−0.3317	−0.4104	−0.4942	−0.6901	−0.9767
$P_{zz,zz}$	−0.4489	−0.6411	−0.7683	−0.8978	−1.1809	−1.5573
$P_{x,x,x}$	−0.3885	−0.8441	−1.2485	−1.7495	−3.1825	−5.8818
$P_{x,x,xx}$	−4.9777	−8.6255	−11.4844	−14.7650	−23.2927	−37.7006
$P_{y,y,xx}$	−0.8024	−1.2178	−1.4983	−1.7856	−2.4135	−3.2287
$P_{z,z,xx}$	−0.9454	−1.5208	−1.9375	−2.3883	−3.4564	−5.0322
$P_{x,y,xy}$	−2.0876	−3.7038	−4.9931	−6.4897	−10.4396	−17.2360
$P_{x,z,xz}$	−1.7504	−2.9683	−3.8945	−4.9326	−7.5295	−11.6704
$P_{x,x,zz}$	−1.0145	−1.6648	−2.1536	−2.6998	−4.0700	−6.2937
$P_{z,z,zz}$	−3.5917	−5.7200	−7.2349	−8.8527	−12.6106	−17.9732

DNC calculations. The effective mass for this vibrational motion is the total mass of the three protons.

Calculations were also carried out to find the electronic–vibrational state properties of H_2 by the same procedure. The x axis was the molecular axis and the properties were evaluated relative to the center of mass.

RESULTS AND DISCUSSION

A comparison of SCF and correlated electrical properties is given in Table IV. The effect of correlation on the second moment elements is small. At equilibrium, the correlation effects are between 0.001 and 0.05 a.u. for all polarizabilities. A polarizability, which is a measure of the electron distribution's readjustment to an external field, is much influenced by the response in the fringe region because that is where the external field is felt the strongest. Since correlation effects on the electron distribution tend to be smaller in regions of lesser electron density, it is not surprising that in this simple system the correlation effect on the polarizability is small. At the $R = 1.15$ a.u. geometry, the range of correlation effects on the polarizabilities is 5%–20%, while at $R = 0.75$ a.u. the range is 0.5%–6%.

TABLE IV. Comparison of SCF and correlated electrical properties[a] of H_3^+.

S' (a.u.)	0.75		1.15	
	DHF	CI	DHF	CI
M_{xx}	−0.5763	−0.5751	−0.9731	−0.9717
M_{zz}	−0.4516	−0.4458	−0.6491	−0.6297
$P_{x,x}$	−2.1800	−2.1607	−5.5122	−5.3972
$P_{z,z}$	−1.5277	−1.4711	−3.0753	−2.7472
$P_{x,xx}$	−0.0707	−0.0750	−0.4524	−0.5385
$P_{xx,xx}$	−0.6156	−0.6128	−2.0862	−2.0953
$P_{xx,yy}$	−0.0679	−0.0634	−0.0361	0.0078
$P_{xx,zz}$	−0.1112	−0.1097	−0.3027	−0.2894
$P_{xy,xy}$	−0.2738	−0.2645	−1.0250	−0.9957
$P_{xz,xz}$	−0.2197	−0.2090	−0.6901	−0.6113
$P_{zz,zz}$	−0.4488	−0.4387	−1.1808	−1.1270

[a] Properties are in a.u. Conventions for properties are discussed in the text.

Table III gives the results of DHF calculations of moments, polarizabilities, and selected hyperpolarizabilities for six D_{3h} geometries. Selected polarizabilities are plotted in Fig. 2. The changes are quite sizable over the range from 0.75 to 1.30 a.u. with the system being much more polarizable when stretched.

The DHF electrical properties of H_2 at equilibrium are given in Table V and compared with the equilibrium values of H_3^+. The polarizabilities of H_3^+ are significantly smaller than those of H_2, with the isotropic dipole polarizability $\bar{\alpha}$ being just about one-third smaller. The spatial delocalization that results from adding the third proton to H_2 could enhance the molecular polarizability, but the greater positive charge leads to a more tightly held, *less* polarizable electron distribution.

Results of the calculations where a single proton was brought into proximity of an equilibrium H_2 molecule are displayed in Fig. 3. The properties were calculated relative to the center of mass of the H_2 molecule with the x axis defined as the line from the proton to the H_2 symmetry center. The interaction of the proton with H_2 is naturally quite long range. This is manifested in the axial x-direction polarizability elements: They begin to increase dramatically when the proton is at $r = 9$ a.u., and then reach a maximum size between 3 and 5 a.u. Energetically, the onset of the interaction is at about 7 a.u. In a very simple physical sense, what is happening at such long distances is just polarization of H_2 by H^+. The interaction energy, at first, is just the energy of polarizing H_2. In a like manner, the enhancement of polarizabilities is, at first, a consequence of the proton's field in

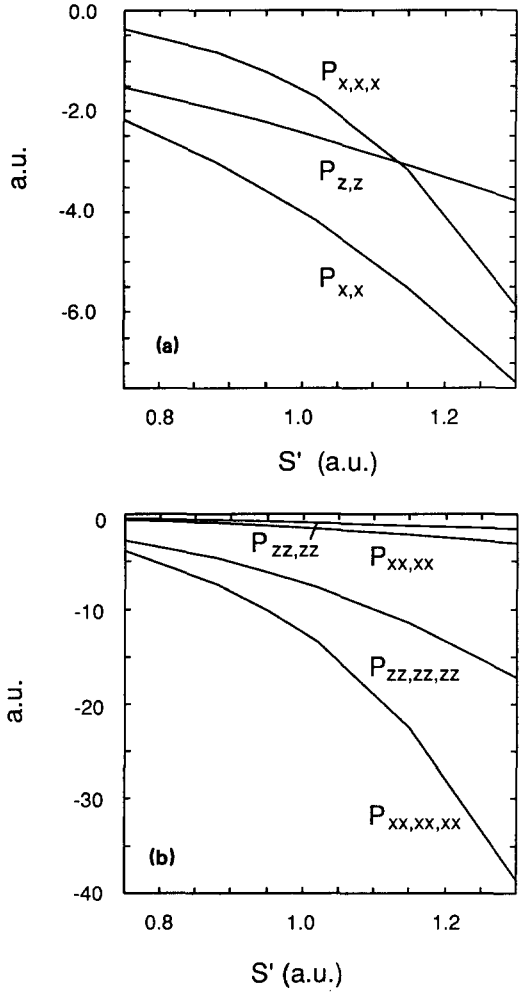

FIG. 2. Electrical properties of H_3^+ in atomic units as a function of symmetric stretching coordinate S'. (a) Dipole polarizability and hyperpolarizability tensor elements. (b) Quadrupole polarizability and hyperpolarizability tensor elements.

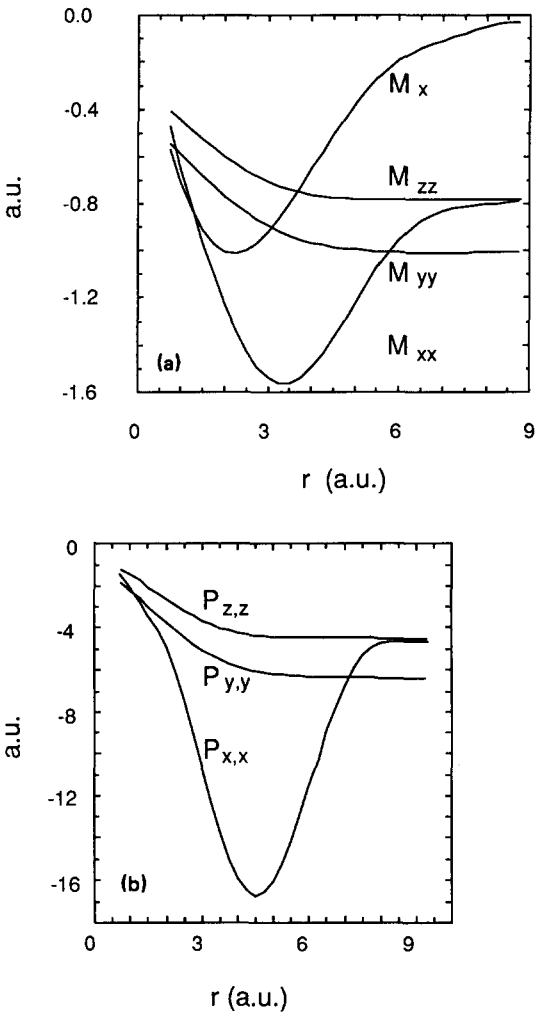

FIG. 3. Electrical properties of H_3^+ as it dissociates to H_2–H^+ in atomic units as a function of r, the distance separating the H_2 center of mass and H^+. H_2 is on the y axis with a bond length of 1.4 a.u. and H^+ is on the x axis. (a) Moment elements. (b) Dipole polarizability elements.

TABLE V. Comparison of equilibrium H_2 and H_3^+ electrical properties (in a.u.) from DHF.

Property[a]	H_2	H_3^+	Ref. 13
M_{xx}	−1.0199	−0.7636	−0.7596
M_{zz}	−0.7772	−0.5517	−0.5418
Θ_{xx}	−0.4856	−0.8476	−0.8716
			−0.8863[b]
$P_{x,x}$	−6.4457	−3.5978	
$P_{z,z}$	−4.4571	−2.2454	
$\overline{\alpha}$[c]	−5.1200	−3.1470	
$P_{x,xx}$	0.0	−0.1977	
$P_{xx,xx}$	−3.6599	−1.1875	
$P_{xx,yy}$	−0.7464	−0.0742	
$P_{xx,zz}$	−0.7464	−0.1911	
$P_{xy,xy}$	−1.2903	−0.5566	
$P_{xz,xz}$	−1.2903	−0.4103	
$P_{yy,yy}$	−1.8769	−1.1875	
$P_{yy,zz}$	−1.8220	−0.1911	
$P_{yz,yz}$	−0.0274	−0.4103	
$P_{zz,zz}$	−1.8769	−0.7683	

[a] For H_2, x is the unique axis, and for H_3^+, z is the unique axis.
[b] Reference 4.
[c] $\overline{\alpha} = 1/3\ (P_{x,x} + P_{y,y} + P_{z,z})$.

concert with the hyperpolarizabilities of H_2 inducing polarizabilities, as in $\alpha^{\text{ind}}_{x,x} = \frac{1}{2}V^2_x\gamma^0_{x,x,x,x}$. The hyperpolarizabilities of H_2 are sizable, as the results given in the Appendix illustrate. As the proton is positioned much closer to H_2, there eventually occurs the electronic structure change leading to bonding to the proton. At that point, the electrons are held *more* tightly and are less polarizable. The permanent moments show similar features. The dipole moment, not counting the contribution of the approaching proton center, reaches a maximum size at about 2.2 a.u. The second moment reaches a maximum at about 3.6 a.u. All the properties vary linearly with the proton's x-coordinate value close to the D_{3h} minimum energy structure; the axial x-direction properties show the sharpest dependence.

Calculations were carried out to characterize the property surfaces more completely than along one dissociation coordinate. Several slices in the S, R, θ space were selected. First, for $\theta = 0°$, calculations were performed on the entire grid of points made up of six values of S (−0.18 to 0.27 in increments of 0.09 a.u.), and seven values of R (−0.3 to 0.3, in increments of 0.1 a.u.). These values were chosen to span a range of energies up to about 6000 cm^{-1} above equilibri-

um. Figure 4 shows the potential energy surface for the region spanned by the grid of points. Figure 5 shows the isotropic in-plane polarizability (the average of $P_{x,x}$ and $P_{y,y}$). This plot shows that the dipole polarizability depends weakly on R, relative to its dependence on S. The out-of-plane dipole polarizability $P_{z,z}$ exhibits a similarly weak dependence on R. Another surface slice was for R fixed at 0.1 a.u. The same S values were used for the grid of points, and seven values of θ were used (0° to 60°, in 10° increments). These values were chosen to span a similar range of energy. As shown in Fig. 6, the in-plane isotropic polarizability depends very weakly on θ. The dependence on S is almost linear. Again, the out-of-plane polarizability behaves similarly.

Since the polarizabilities show such weak dependence on R and θ, it is reasonable to approximate the electrical properties as being functions only of S. This means that much of the vibrational contribution to the properties comes from the symmetric stretch. An assessment of the size of that

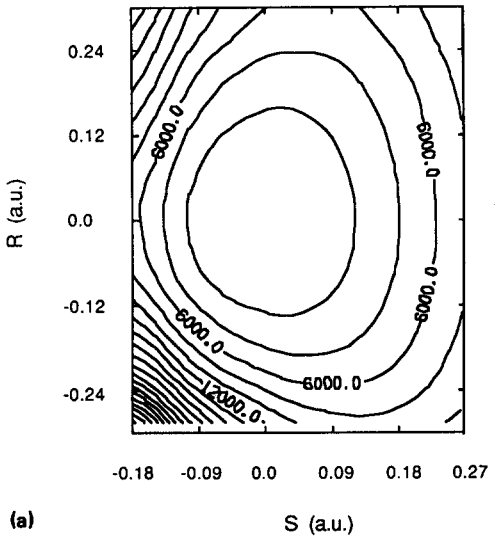

(a)

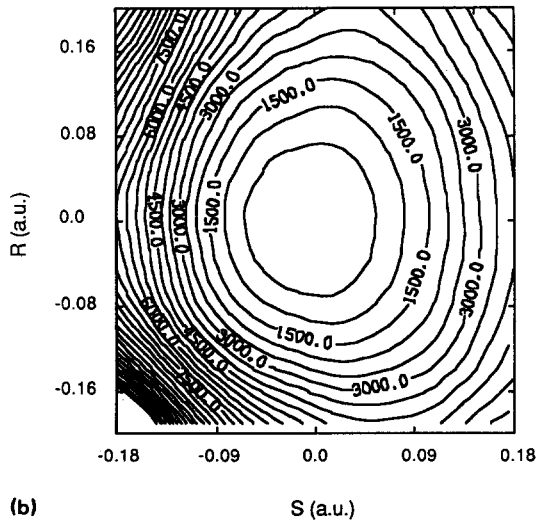

(b)

FIG. 4. Potential energy contour plots of H_3^+ as a function of the symmetric stretching displacement S (a.u.), and the asymmetric displacement R (a.u.) with the displacement angle $\theta = 0$ deg. (a) Relative energy $(E - E_{eq})$ in cm^{-1}, with contours of 2000 cm^{-1}. (b) Relative energy $(E - E_{eq})$ in cm^{-1}, with contours of 500 cm^{-1}.

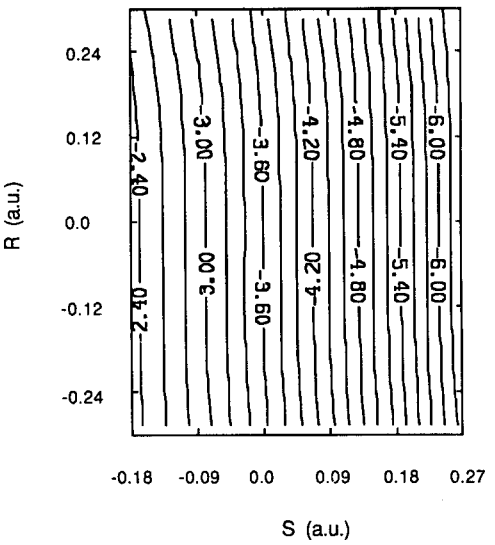

FIG. 5. Contour plots of the isotropic in-plane polarizability $(P_{x,x} + P_{y,y})/2$ of H_3^+ as a function of the symmetric stretching displacement S (a.u.) and the asymmetric displacement R (a.u.) with the displacement angle fixed at $\theta = 0$ deg.

contribution, with the molecule frozen to rotation, was obtained from the derivative Numerov Cooley (DNC) calculations on the pure symmetric stretch vibrational levels. Table VI gives the unique elements of the derivative properties of the electronic state at equilibrium, of the ground vibrational state, and of the first two excited, symmetric stretch states. The vibrational state moments, dipole polarizability, and the dipole–quadrupole polarizability are the same as the vibrational averages of the corresponding electronic properties.[31,33] Generally, the properties increase with vibrational excitation. The in-plane dipole polarizability is over 25% larger for the second excited state than for the ground state. The primary reason why this happens is that the vibrational excursions in the higher states sample more of the distorted

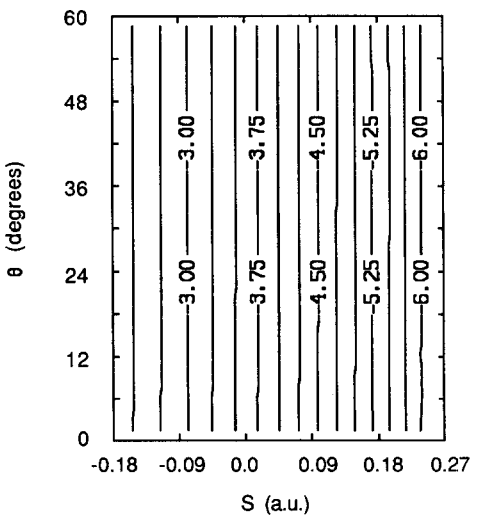

FIG. 6. Contour plots of the isotropic in-plane polarizability $(P_{x,x} + P_{y,y})/2$ of H_3^+ as a function of the symmetric stretching displacement S (a.u.) and the displacement angle θ (deg), with the asymmetric displacement coordinate fixed at $R = 0.1$ a.u.

TABLE VI. Vibrational state electrical properties of H_2 and H_3^+.

Property	H_3^+				H_2			
	Equil.	$v=0$	$v=1$	$v=2$	Equil.	$v=0$	$v=1$	$v=2$
M_{xx}	−0.7636	−0.7816	−0.8178	−0.8556	−1.0200	−1.0603	−1.1464	−1.2687
M_{zz}	−0.5517	−0.5597	−0.5751	−0.5909	−0.7772	−0.7925	−0.8233	−0.8651
$P_{x,x}$	−3.5978	−3.7705	−4.1346	−4.5231	−6.4458	−6.8941	−7.8760	−9.2948
$P_{z,z}$	−2.2454	−2.3187	−2.4623	−2.6128	−4.4571	−4.6220	−4.9569	−5.4212
$\overline{\alpha}$[a]	−3.1470	−3.2866	−3.5772	−3.8863	−5.1200	−5.3793	−5.9299	−6.7124
$P_{x,xx}$	−0.1978	−0.2206	−0.2797	−0.3444	0.0000	0.0000	0.0000	0.0000
$P_{xx,xx}$	−1.1875	−0.4796	−0.5438	−0.5960	−3.6599	−2.3742	−2.3628	−0.6166
$P_{xx,yy}$	−0.0743	0.7185	0.8535	1.0174	−0.7464	−0.1218	−0.0157	0.7111
$P_{xx,zz}$	−0.1911	0.1833	0.2060	0.2368	−0.7464	−0.1218	−0.0157	0.7111
$P_{xy,xy}$	−0.5566	−0.5991	−0.6986	−0.8067	−1.2904	−1.3874	−1.5989	−1.9040
$P_{xz,xz}$	−0.4104	−0.4361	−0.4911	−0.5502	−1.2904	−1.3874	−1.5989	−1.9040
$P_{yy,zz}$	−0.1911	0.1833	0.2060	0.2368	−1.8220	−1.6514	−1.8364	−1.9076
$P_{yz,yz}$	−0.4104	−0.4361	−0.4911	−0.5502	−0.0275	−0.0274	−0.0272	−0.0267
$P_{zz,zz}$	−0.7683	−0.6186	−0.6789	−0.7401	−1.8770	−1.7062	−1.8907	−1.9609
$P_{x,x,x,x}$	−58.744	−241.63	−299.33	−368.97	−506.18	−1086.1	−1428.8	−1900.9
$P_{x,x,z,z}$	−21.255	−49.988	−60.332	−86.011	−132.99	−217.01	−265.17	−326.56
$P_{z,z,z,z}$	−45.652	−85.293	−98.193	−112.91	−127.81	−220.96	−246.96	−280.72

[a] $\overline{\alpha} = (P_{x,x} + P_{y,y} + P_{z,z})/3$.

regions where the pure electronic polarizabilities are bigger. The vibrational contributions evaluated here presume a field source rotating with the molecule, as would be the case if H_3^+ were in a weak complex with some other molecule and it was the charge field of that molecule that was electrically perturbing H_3^+. A freely rotating H_3^+ in a laboratory-fixed frame is a different situation, and corresponding polarizability evaluations should account for rotation as well as vibration.[34,35]

Values for the vibrational state properties of H_2, neglecting rotation, are given in Table VI for comparison with the H_3^+ properties. In H_2, vibrational motion has a greater percentage effect on the dipole polarizability than in H_3^+. It is also quite interesting that the dipole second hyperpolarizability of H_3^+ is much smaller than that of H_2. In many ways, then, the electrical "picture" of H_3^+ is easier to construct. Because the excess positive charge makes it less polarizable, there is both better convergence in the polarizability expansion (i.e., smaller hyperpolarizabilities), and less error from neglect of vibrational contributions.

ACKNOWLEDGMENTS

This work was supported in part by the Physical Chemistry Program of the National Science Foundation (Grant CHE 84-19496). Many of the calculations were carried out on the Cray supercomputer at the National Center for Supercomputing Applications, Urbana, Illinois.

APPENDIX

Because H_2 and H_3^+ are such simple systems, they are good cases for assessing if there are differences in basis set effects on polarizabilities between the neutral and the charged species. Some differences are expected because of the contraction of charge around each nucleus in the cation. Likewise, one would expect differences of the opposite sort in H_3^-.

The basis set tests that were carried out were DHF evaluations of the dipole polarizability (α), hyperpolarizability (β), and second hyperpolarizability (γ) at equilibrium. Higher multipole polarizabilities may exhibit a somewhat different dependence on basis set size. The primary aim was to compare how diffuse the *s,p,d* shell basis functions needed to be, and this could be specific for one multipole's polarizabilities. Evaluation of higher multipole properties was carried out with the largest basis set for both H_2 and H_3^+. The sets tested are rather sizable for hydrogen, with the largest having 40 functions per atom. It should be pointed out that with larger molecules, polarization comes about partly through interatomic valence readjustment, and accurate values can often be obtained with more conservative bases[36] than those used here.

Basis sets of various sizes were constructed by augmenting the *s*-shell basis (given in Table I) with uncontracted *s*, *p*, and *d* functions. Linear dependencies were removed from the basis. Most calculations were done on H_2, because as expected, its properties showed greater sensitivity to the basis than did the properties of H_3^+. These tests on H_2 are similar but more extensive than those already reported.[26] Three factors were adjusted in the augmenting functions. For each *l* shell, these factors were the number of functions, the value of the largest (or smallest) exponent, and the ratio of one exponent to the next. The results in Table VII show that convergence is easily accomplished for the dipole polarizability of H_2 but is slower for the second hyperpolarizabilities. In contrast, convergence is very rapid for H_3^+, and that is shown by the results in Table VIII.

The calculations on H_2 with basis sets 20A–F test the

TABLE VII. Basis set test results for H_2.

Basis set designation	Number of basis functions	Exponents of uncontracted functions			$P_{x,x}$	$P_{z,z}$	$P_{x,x,x,x}$	$P_{x,x,y,y}$	$P_{y,y,z,z}$	$P_{z,z,z,z}$
		s	p	d						
20A	40		1.6 0.5 0.15	1.33	−6.446	−4.457	−506.2	−133.0	−42.60	−127.8
20B	40		1.6 0.5 0.15	0.10	−6.453	−4.457	−634.2	−151.3	−90.40	−271.2
20C	40		1.6 0.5 0.15	0.08	−6.453	−4.455	−641.9	−146.5	−85.95	−257.8
20D	40		1.6 0.5 0.15	0.06	−6.449	−4.462	−645.0	−134.2	−80.95	−242.9
20E	40		1.6 0.5 0.15	0.04	−6.445	−4.488	−631.3	−126.7	−81.29	−243.9
20F	40		1.6 0.5 0.15	0.02	−6.442	−4.505	−559.8	−131.6	−80.59	−241.8
20G	40		1.6 0.4 0.1	0.08	−6.451	−4.591	−637.2	−196.2	−176.3	−528.8
20H	40		1.6 0.32 0.064	0.08	−6.445	−4.497	−636.2	−196.2	−237.7	−713.1
20I	40		1.6 0.29 0.053	0.08	−6.443	−4.447	−637.4	−187.9	−233.3	−700.0
20J	40		1.6 0.27 0.044	0.08	−6.442	−4.392	−639.4	−177.7	−216.7	−650.1
30A	60	0.02	1.6 0.32 0.064 0.0128	0.08 0.016	−6.446	−4.513	−642.2	−198.4	−228.6	−685.7
40A	80	0.023 0.006	1.6 0.032 0.064 0.0128 0.0025	0.08 0.016 0.0032	−6.446	−4.514	−642.6	−198.7	−228.6	−685.8

effect of varying the d exponent. A small exponent is important for the polarizabilities. Calculations with basis sets 20G–J test the effect of varying the ratio of the p-function exponents. A ratio of five (basis 20H) yielded the greatest overall influence of the p functions on the properties. A higher or lower ratio, with the largest exponent held at 1.6, yielded a lesser role for the p functions, and so 20H was considered the best. The ratio of five is in line with the ratios suggested as being best for polarizability evaluations by Werner and Meyer[37] and Christiansen and McCullough.[38] Also, a series of calculations, not listed in Table VII, were carried out varying the d exponent by otherwise using basis 20H, and this showed that a value of 0.08 maximized the overall importance of the d function.

Two further tests were performed by enlarging the 20H basis with one and two more sets of functions. Earlier studies on H_2[26] indicated that a balance between the flexibility in each l shell is important and that for hydrogen, this balance could be achieved if there were N-2l functions for each l shell (e.g., for $N=4$ [4s2p], for $N=5$ [5s3p1d], for $N=6$ [6s4p2d]). On that basis and with the optimum exponent ratio of five, basis sets 30A and 40A were constructed. The differences between 20H and 30A are at most a few percent, while the differences between 30A and 40A are unimpor-

TABLE VIII. Basis set test results for H_3^+.

Basis set designation	Number of basis functions	Exponents of uncontracted functions			$P_{x,x}$	$P_{z,z}$	$P_{x,x,x}$	$P_{x,x,x,x}$	$P_{x,x,y,y}$	$P_{y,y,z,z}$	$P_{z,z,z,z}$
		s	*p*	*d*							
20A	60		1.6 0.5 0.15	1.33	−3.598	−2.245	−1.249	−58.74	−19.58	−21.26	−45.65
20H	60		1.6 0.32 0.06	0.08	−3.594	−2.231	−1.244	−59.90	−19.97	−18.17	−54.83
30A	90	0.02	1.6 0.32 0.064 0.0128	0.08 0.016	−3.595	−2.236	−1.243	−60.20	−20.07	−18.66	−54.57
40A	120	0.023 0.006	1.6 0.032 0.064 0.0128 0.0025	0.08 0.016 0.0032	−3.595	−2.236	−1.244	−60.25	−20.08	−18.69	−54.58

tant. The H_3^+ results in Table VIII show very small differences between the primary basis, 20A, and these larger sets. There is very little sensitivity to the *d*-function exponent, and generally, the cation has much smaller basis set demands. The use of the basis in Table I will be least accurate at the far separation distances of H^+ interacting with H_2, but the likely errors will not be important in the relative changes along this path.

TABLE IX. Equilibrium H_2 and H_3^+ DHF electrical properties (in a.u.) from basis 40A.

Property[a]	H_2	Ref. 28[b]	Ref. 25[c]	H_3^+
M_{xx}	−1.0197			−0.7639
M_{zz}	−0.7773			−0.5531
Θ_{xx}	−0.4848	−0.4953	−0.4865	−0.8432
$P_{x,x}$	−6.4454	−6.45		−3.5949
$P_{z,z}$	−4.5074	−4.47		−2.2357
$\overline{\alpha}$[c]	−5.1534	−5.13		−3.1418
$P_{x,xx}$	0.0			−0.1952
$P_{xx,xx}$	−3.8834			−1.2237
$P_{xx,yy}$	−0.6615			−0.1004
$P_{xx,zz}$	−0.6615			−0.1895
$P_{xy,xy}$	−1.4015			−0.5616
$P_{xz,xz}$	−1.4015			−0.4110
$P_{yy,yy}$	−2.9091			−1.2237
$P_{yy,zz}$	−0.8744			−0.1895
$P_{yz,yz}$	−1.0174			−0.4110
$P_{zz,zz}$	−2.9091			−0.7841
$C_{xx,xx}$	5.9361	6.06	5.92	
$C_{xz,xz}$	4.2045	4.23	4.23	
$C_{zz,zz}$	4.5361	5.05	4.58	
$P_{x,x,x,x}$	−642.6	−683		−60.25
$P_{x,x,y,y}$	−198.7	−214		−20.08
$P_{y,y,z,z}$	−228.6			−18.68
$P_{z,z,z,z}$	−685.8	−704		−54.58

[a] For H_2, *x* is the unique axis, and for H_3^+, *z* is the unique axis.

[b] For this fixed charge calculation, $R = 1.401\,146$ and the basis size was (11*s*5*p*2*d*/8*s*5*p*2*d*).

[c] This calculation was carried out with the finite field method, using a (7*s*2*p*1*d*/4*s*2*p*1*d*) basis.

[d] $\overline{\alpha} = 1/3(P_{x,x} + P_{y,y} + P_{z,z})$.

Table IX lists all polarizabilities studied here from using the largest basis in Table VII. Diercksen and Sadlej[25] obtained SCF level results for the quadrupole moment and polarizability that are very similar to the results obtained here. They used a (7*s*2*p*1*d*/4*s*2*p*1*d*) contracted set where the *d* exponent was 0.075 and was optimized for the quadrupole polarizability. Maroulis and Bishop[28] carried out fixed charge calculations using an (11*s*5*p*2*d*/8*s*5*p*2*d*) contracted set, and the biggest disagreement in values is 10%, for $C_{zz,zz}$.

The values for quadrupole polarizabilities of H_3^+ with the 40A basis are little different from the corresponding results obtained from the smaller 20A basis of Table I. It is quite apparent, then, that basis set requirements for finding electrical properties may be much easier to meet for a cation than for a neutral, or worse, an anion.

[1] G. D. Carney and R. N. Porter, J. Chem. Phys. **65**, 3547 (1976).
[2] C. E. Dykstra and W. C. Swope, J. Chem. Phys. **70**, 1 (1979). As noted elsewhere point #56 was incorrectly listed. The energy for this point should be −0.887 492 a.u.
[3] P. G. Burton, E. Von Nagy-Felsobuki, G. Doherty, and M. Hamilton, Mol. Phys. **55**, 527 (1985).
[4] W. Meyer, P. Botschwina, and P. Burton, J. Chem. Phys. **84**, 891 (1986).
[5] T. Oka, Phys. Lett. **45**, 531 (1980).
[6] G. D. Carney and R. N. Porter, Chem. Phys. Lett. **50**, 327 (1977).
[7] G. D. Carney, Mol. Phys. **39**, 923 (1980).
[8] G. D. Carney, S. M. Alder-Golden, and D. C. Lessesi, J. Chem. Phys. **84**, 3921 (1985).
[9] B. Martire and P. G. Burton, Chem. Phys. Lett. **121**, 479 (1985).
[10] J. Tennyson and B. Sutcliffe, Mol. Phys. **51**, 887 (1984).
[11] I. Hamilton, J. Chem. Phys. **87**, 774 (1987).
[12] K. G. Lubic and T. Amano, Can. J. Phys. **62**, 1886 (1984).
[13] G. D. Carney and R. N. Porter, J. Chem. Phys. **60**, 4251 (1974).
[14] W. Kolos and C. C. J. Roothan, Rev. Mod. Phys. **32**, 219 (1960).
[15] W. Kolos and L. Wolniewicz, J. Chem. Phys. **41**, 3674 (1964).
[16] L. Wolniewicz, J. Chem. Phys. **45**, 515 (1966).
[17] W. Kolos and L. Wolniewicz, J. Chem. Phys. **46**, 1426 (1967).

[18]J. Rychlewski, Mol. Phys. **41**, 833 (1980).
[19]D. M. Bishop and L. M. Cheung, J. Chem. Phys. **72**, 5125 (1980).
[20]D. M. Bishop and B. Lam, Chem. Phys. Lett. **134**, 283 (1987).
[21]W. Meyer, Chem. Phys. **17**, 27 (1976).
[22]E. A. McCullough, Jr., J. Chem. Phys. **63**, 5050 (1975).
[23]M. Jaszunski and B. O. Roos, Mol. Phys. **52**, 1209 (1984).
[24]K. Szalewicz, L. Adamowicz, and A. J. Sadlej, Chem. Phys. Lett. **61**, 548 (1979).
[25]G. H. F. Diercksen and A. J. Sadlej, Theor. Chim. Acta. **63**, 69 (1983).
[26]C. E. Dykstra, J. Chem. Phys. **82**, 4120 (1985).
[27]C. E. Dykstra and P. G. Jasien, Chem. Phys. Lett. **109**, 388 (1984).
[28]G. Maroulis and D. Bishop, Chem. Phys. Lett. **128**, 462 (1986).
[29]S. Huzinaga, J. Chem. Phys. **42**, 1293 (1965).
[30]W. Meyer, J. Chem. Phys. **64**, 2901 (1976); C. E. Dykstra, H. F. Schaefer, and W. Meyer, *ibid.* **65**, 2740 (1976).
[31]C. E. Dykstra, S. Y. Liu, and D. J. Malik, Adv. Chem. Phys. (in press).
[32]J. Applequist, Chem. Phys. **85**, 279 (1984).
[33]C. E. Dykstra and D. J. Malik, J. Chem. Phys. **87**, 2806 (1987).
[34]M. Brieger, Chem. Phys. **89**, 275 (1984).
[35]D. M. Bishop, B. Lam, and S. T. Epstein, J. Chem. Phys. **88**, 337 (1988).
[36]S.-Y. Liu and C. E. Dykstra, Chem. Phys. Lett. **119**, 407 (1985).
[37]H.-J. Werner and W. Meyer, Mol. Phys. **31**, 855 (1976).
[38]P. A. Christiansen and E. A. McCullough, Chem. Phys. Lett. **55**, 439 (1978).